Post-Print Version

Original version: https://doi.org/10.1016/j.ijfatigue.2013.11.023

On Long-Term Fatigue Damage and Reliability Analysis of Gears under Wind Loads in Offshore Wind Turbine Drivetrains

Amir Rasekhi Nejad, Zhen Gao, Torgeir Moan
Norwegian Research Centre for Offshore Wind Technology (Nowitech) and
Centre for Ships and Ocean Structures (CeSOS)
Norwegian University of Science & Technology (NTNU), Trondheim, Norway

Corresponding author: Amir.Nejad@ntnu.no, Tel: +47 73591546, Fax: +47 73595528

Mailing address: Centre for Ships and Ocean Structures (CeSOS), Norwegian University of Science and Technology (NTNU), Otto Nielsens V.10, N-7491, Trondheim, Norway

Abstract

In this paper, a long-term fatigue damage analysis method for gear tooth root bending in wind turbine's drivetrains is presented. The proposed method is established based on the ISO gear design codes which are basically developed for gears in general applications, not specifically for wind turbine gears. The ISO procedure is adapted and further improved to include the long-term fatigue damage of wind turbine's gears. The load duration distribution (LDD) method is used to obtain the short-term stress cycles from the input load time series of global response analysis. Dynamic loads and load effects in the gearbox are obtained by two dynamic models; a simplified approach and Multi Body Simulation (MBS) method. A good agreement between these two methods is observed. The long-term fatigue damage is then calculated based on the SN-curve approach by considering all short-term damages and the long-term wind speed distribution. Finally, the reliability and service life probability of failure considering load and load effect uncertainties is calculated. The procedure is exemplified by a 5 MW gearbox designed for a pitch controlled, bottom-fixed offshore wind turbine.

Key words: wind turbine gears; long-term fatigue; drivetrains; reliability

1. Introduction

The recent developments in drivetrain technologies have brought a wide range of options for wind energy industry. Alongside the dominant high ratio gearboxes, medium ratio gear trains, direct drives, hydraulic drives, differential and variable speed gearboxes are available commercially in the wind turbine market. Yet, the majority (90%) of drivetrains in currently

installed turbines are based on gear technology [1]. The wind turbine gearbox failure investigations carried out by Musial et al. [2] indicate that the design process may have the biggest contribution to the premature failures of wind turbine gearboxes. The first wind turbine gearbox design code, ISO 81400-4 [3] was issued in 2005 and replaced by the extensively modified IEC 61400-4 standard [4] recently in December 2012. According to this design code, the gears in wind turbines shall be designed based on ISO 6336 [5-9] series for calculation of the gear load capacity. The ISO 6336 design procedures are for gears in general applications and are not customized for any specific usage. Thus, the IEC 61400-4 has set the minimum level of safety factors which should be considered while following ISO 6336 procedures for wind turbine applications. It is, however, unknown what level of reliability can be achieved by using the IEC safety factors.

Part 6 of ISO 6336 [9] – the newest part in the 6336 series with first edition issued in 2006 - covers the calculation of gearbox service life under variable loads for general applications. In order to use the ISO 6336-6 for wind turbine gears, further improvements and adaptations are required. In ISO 6336-6 or IEC 61400-4, no procedure for the long-term fatigue damage calculation is offered. There are few publications about the fatigue analysis of wind turbine gears in which only the short-term fatigue is addressed [10,11].

The stress range and fatigue cycle counting have also their own challenges in wind turbine gears. The load response or stress range for gears is fundamentally different than shafts or other components in the gearbox. In every rotation, a single tooth undergoes root bending or surface pitting stress ranging from zero to a certain peak value which does not explicitly correspond to the input load fluctuations. This is due to the fact that the gear stress range is not only a function of the external load fluctuations but also it is a function of gear rotational speed. In wind turbines, the stress range for different gear stages should be established by taking into account both load and speed variations. Therefore, the stress cycle counting method for gears is not the same as for structural components [4].

In order to overcome the problem with the stress range and cycle counting, the load duration distribution (LDD) method which is based on the stress bins, is recommended by IEC 61400-4. The number of stress bins influences the calculated fatigue damage, thus it is important to establish a minimum level for the bin numbers in wind turbine gear design.

In this paper, a long-term fatigue damage calculation method for gears in wind turbine drivetrains is proposed. The method is developed based on the ISO 6336-6 and is customized for wind turbine gears rather than for gears in general applications. The reliability of the gears designed by this method is then calculated by the structural reliability approach considering the load, load effect, and resistance uncertainties. The scope of the paper is limited to the gear tooth root bending fatigue, though the procedure described herein can be used for the pitting damage calculation of gears provided that related gear surface stress equations are used. The method is exemplified by a 5 MW gearbox designed for a bottom-fixed offshore wind turbine.

2. Long-term environmental condition and global analysis

The wind load is the only environmental load considered in this study. Since the wind turbine is bottom-fixed, the influence of wave loads on the drivetrain response can be neglected. The probability density function of 1-h mean wind speed at 10 m above the average sea level is modelled by the 2-parameter Weibull distribution [12,13]:

$$F_U(u) = 1 - \exp\left[-\left(\frac{u}{a}\right)^c\right] \quad (1)$$

a and c are the shape and scale parameters which, for instance, are 8.426 and 1.708 for Northern North sea respectively [12]. The wind speed at hub height is calculated from the power law, with the power value of 0.14 for offshore fields [14]:

$$u_{hub} = u\left(\frac{h_{hub}}{10}\right)^{0.14} \quad (2)$$

It should be noted that the cut-in, rated and cut-out wind speeds given in the wind turbine specifications refer to the wind speed at the nacelle height, 90 m above the average sea level [15].

A decoupled analysis method is used to estimate the drivetrain dynamic response from the environmental load, i.e. the wind load. The global analysis is performed first, using the aero-servo-elastic code HAWC2 [16], followed by a local analysis of the drivetrain using a simplified method and considering the main shaft torque from the global HAWC2 analysis as input. The response analyses are carried out considering the long-term input loading. In order to minimize the statistical uncertainties, 15 simulations are carried out for each wind speed over 800 sec. and the first 200 sec. is removed to avoid start-up transient effects. The

reference turbulence intensity factor is taken as 0.14 for all the wind speeds, according to IEC 61400-1 class B turbine.

3. 5 MW case study gearbox

In this study, a 5 MW gearbox has been designed and utilized to demonstrate the proposed procedure. The gearbox configuration follows the common wind turbine designs with three stages, two planetary gears and one helical gear pair. In order to avoid complexities with respect to the load sharing behaviour between planets [17], the planetary stages are designed with three planets. The turbine data are taken from NREL 5 MW fixed offshore reference turbine, presented in Table 1 [18]. For any wind turbine design, there is always more than a single gearbox solution. In practice, apart from the minimum requirements set by design codes, many project-specific factors such as installation issues, weight, manufacturing limitation and material availability influence the gearbox design. The gearbox in this paper is intended to illustrate the gear fatigue design procedure and no optimization with respect to the weight and size is considered. Figures 1,2 and Tables 2,3 present the gearbox layout, topology and technical data. All data are provided; thus, one can replicate the proposed procedure through the given example and employ the method for industrial applications.

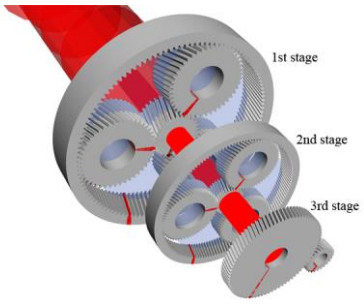

Fig. 1: Three-stage gearbox for 5MW wind turbine.

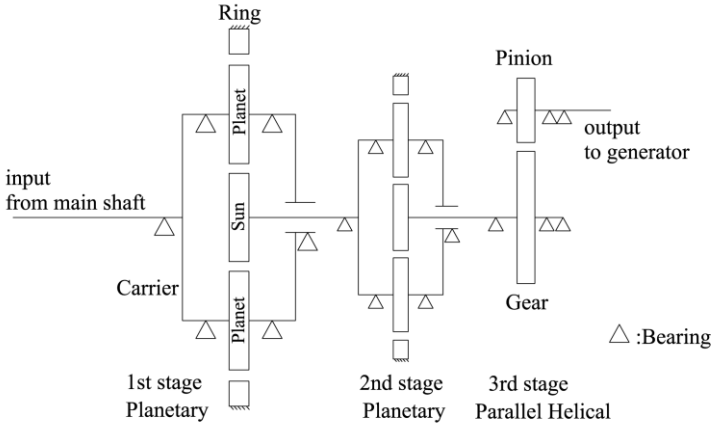

Fig. 2: Topology of the 5MW gearbox.

Table 1: 5 MW NREL reference wind turbine [18].

Rated power (MW)	5
Cut-in wind speed (m/sec)	3
Cut-out wind speed (m/sec)	25
Rated wind speed (m/sec)	11.4
Rated rotor speed (rpm)	12.1
Hub height, above mean sea level	90
Rotor diameter (m)	126
Power control system	Pitch

Table 2: 5 MW gearbox specifications.

Type	2P+1H
Ratio	1:97.20
Designed power (kW)	5000
Rated generator speed (rpm)	1173.7
Service life (year)	20

P: Planetary, H: Parallel Helical

Table 3: 5 MW gear data.

		1st stage	2nd stage	3rd stage
Type		Planetary	Planetary	Helical
Ratio		1:5.17	1:5.80	1:3.24
Number of planets		3	3	-
Normal Module (mm)		22	12	14
Normal Pressure angle (degree)		20	20	20
Helix angle (degree)		15	15	15
Face width (mm)		620	459	329
Centre distance (mm)		857	541	781
Number of teeth	Sun gear	29	30	-
	Planet/pinion	46	57	25
	Ring/gear	121	144	81
Profile shift coefficient	Sun gear	-0.23	-0.33	-
	Planet/pinion	0.36	0.38	0.44
	Ring/gear	-0.50	-0.43	0.52

4. Long-term gear tooth root bending fatigue

The aim of the ISO 6336-6 standard is primarily to evaluate the safety factor of an existing design against fatigue damage under variable loads. The ISO procedure starts with establishing torque bins from the input torque time series and calculating the stress bins based on the upper level of each torque bins. The fatigue damage is then obtained from the Palmgren-Miner hypothesis of linear damage and gear SN curve data. The iteration to calculate the safety factor (S_F) continues until the damage is within the range of 0.99 to 1.0.

In Fig. 3 a customized version of ISO 6336-6 method for long-term fatigue design of wind turbine gears under variable wind loads is proposed. The initial values of gear main parameters such as normal module, pressure angle, facewidth, helix angle, number of teeth and material are estimated by methods specified by ISO 6336-2 and 3 based on the ultimate load in the load bins. In this paper, the fatigue criterion is fulfilled by varying the gear facewidth; however, one can iterate other design parameters such as gear material, heat treatment, module, pressure angle and other basic parameters. In following sections the steps of this modified ISO 6336-6 procedure are discussed and exemplified by a 5 MW case study gearbox.

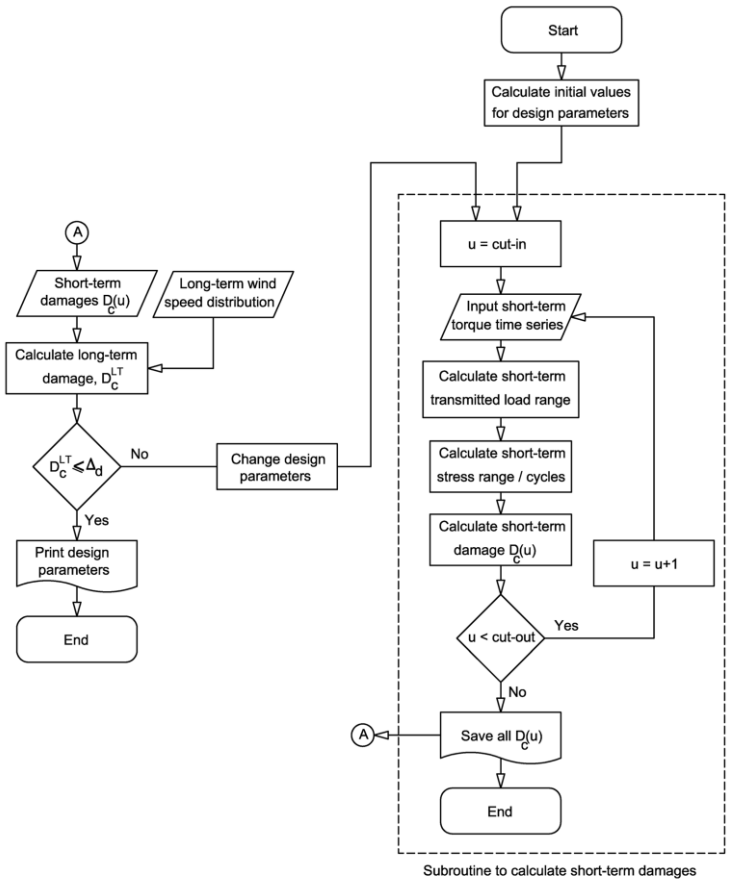

Fig. 3: Proposed modified ISO 6336-6 procedure for wind turbine gear design with respect to the long-term fatigue damage.

4.1- Short-term load range

The input load on the wind turbine gearbox is obtained from numerical simulations or from test results covering the operational wind speeds. It is a common practice to limit the gearbox

input load to the main shaft torque and assume that all the non-torque loadings are filtered by bearings before reaching to the gears. This assumption is not valid for all design types of wind turbine gearboxes and should be evaluated on a case-by-case basis. The non-torque loads can influence the gear load spectra as shown by Xing and Moan [19].

The gear mesh force or transmitted load can be obtained directly from the input torque by analytical methods or by multibody model simulations [20,21] which are detailed in following sections. The transmitted load F^t is the resultant load from the applied torque on gear and is the cause for bending stress in gear tooth root fillet.

4.1.1- Multibody Simulation (MBS) method

In the MBS method, the gearbox is modelled as a system of rigid or flexible bodies interconnected with appropriate joints. The application of MBS model in wind turbine drivetrains is proven by comparison with FEM and experimental results [11,19,21,22].

Parker et al. [23] indicated that the elastic deformations of the gears are much smaller than the rigid body motions and thus they can be superposed. The $\mathbf{x}_{fi}$,displacement vector of component i, can be expressed by linear system of differential equations [23,24]:

$$\mathbf{M}_{fi}\ddot{\mathbf{x}}_{fi} + \mathbf{C}_{fi}\dot{\mathbf{x}}_{fi} + \mathbf{K}_{fi}\mathbf{x}_{fi} = \mathbf{f}_{fi} \tag{3}$$

in which $\mathbf{f}_{fi}$ is the external force vector, including moments and torques and $\mathbf{M}$, $\mathbf{C}$ and $\mathbf{K}$ are inertia, damping and stiffness matrix respectively. They also include gear tooth stiffness and damping. If $\mathbf{x}_{ri}$ represents the rigid body motion of reference frame of component i, the overall equation of motion can be written as:

$$\begin{bmatrix} \mathbf{M}_{fi} & \mathbf{M}_{fri} \\ \mathbf{M}_{rfi} & \mathbf{M}_{ri} \end{bmatrix} \begin{Bmatrix} \ddot{\mathbf{x}}_{fi} \\ \ddot{\mathbf{x}}_{ri} \end{Bmatrix} + \begin{bmatrix} \mathbf{C}_{fi} & \mathbf{C}_{fri} \\ \mathbf{C}_{rfi} & \mathbf{C}_{ri} \end{bmatrix} \begin{Bmatrix} \dot{\mathbf{x}}_{fi} \\ \dot{\mathbf{x}}_{ri} \end{Bmatrix} + \begin{bmatrix} \mathbf{K}_{fi} & \mathbf{K}_{fri} \\ \mathbf{K}_{rfi} & \mathbf{K}_{ri} \end{bmatrix} \begin{Bmatrix} \mathbf{x}_{fi} \\ \mathbf{x}_{ri} \end{Bmatrix} = \begin{Bmatrix} \mathbf{f}_{fi} \\ \mathbf{f}_{ri} \end{Bmatrix} \tag{4}$$

The motion equation of entire drivetrain is then expressed as [23]:

$$\mathbf{M}\ddot{\mathbf{x}} + \mathbf{C}\dot{\mathbf{x}} + \mathbf{K}\mathbf{x} = \mathbf{F} \tag{5}$$

The Newmark method can be used for time integration of the above equations [23-25] or MBS software such as SIMPACK [26] can be employed. SIMPACK is a multi-purpose multibody simulation code with features available to model gearboxes. The main shaft torque

is applied at the end of the main shaft where the rotor hub is connected while the generator speed is controlled on the other side of the gearbox.

The advantage of the MBS method is that dynamic effects of components are automatically included in the analysis. Moreover non-torque forces and moments can be added to the input loadings. Nevertheless, the accuracy of the results is directly dependent on the precision of the given stiffness, inertia and damping values.

The 5 MW case study gearbox is modelled by the MBS method. Fig. 4 shows the first stage MBS model kinematic topology and force elements used in SIMPACK. The modelling follows the procedure used to study the NREL gearbox reliability collaborative (GRC) model and validated by experimental results [27].

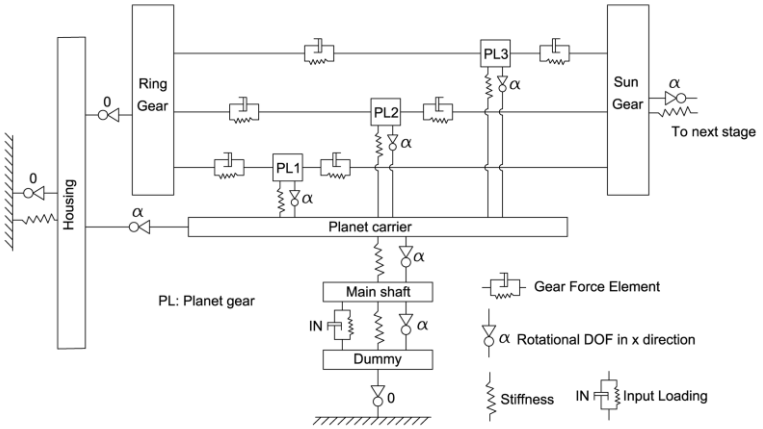

Fig. 4: MBS topology of 5 MW gearbox's first stage.

4.1.2- Simplified gear load analysis method

The simplified method is used in the early design stage when the stiffness and damping parameters of gearbox components are often unknown. The idea behind this method is to calculate gear load directly from a global load model using a simplified quasi-static analysis while considering the associated uncertainties. The problem is simplified by assuming that gear bodies are rigid and their interaction is through rigid contacts with zero damping. If the internal gear dynamic effect is neglected, the interaction force between two gears is calculated directly from the external forces.

The equation of motion for the main shaft, gearbox and generator in a simplified dynamic model can be obtained from lumped mass method – shown in Fig. 5.

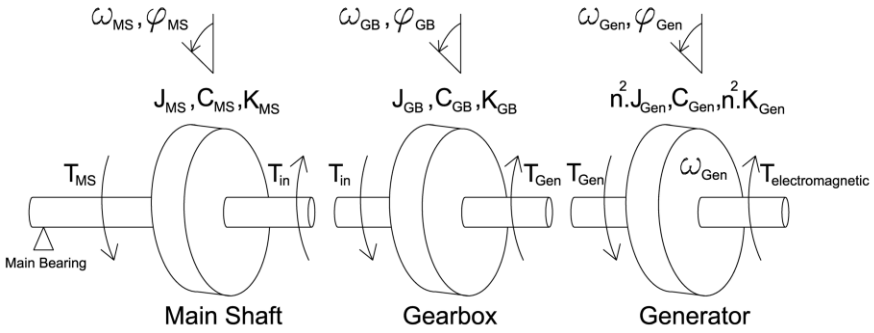

Fig. 5: Lumped mass model of main shaft, gearbox and generator (n is gearbox ratio).

T_{in} , the input torque for the gearbox, is calculated from the main shaft equation of motion:

$$T_{in} = \left(T_{MS} - \left(J_{MS} \frac{d\omega_{MS}}{dt} + C_{MS}\omega_{MS} + K_{MS}\varphi_{MS} \right) \right) \approx T_{MS} - J_{MS} \frac{d\omega_{MS}}{dt} \tag{6}$$

J_{MS}, C_{MS} and K_{MS} are torsional moment of inertia, damping and stiffness of main shaft. T_{MS} and ω_{MS} are the main shaft torque and angular velocity which are known from the global response simulation.

For a pair of gears in contact, the transmitted force including all gear dynamic models [28,29] leads to a form like:

$$F^t = \frac{2}{d_1} \left(T_{in} - \left(J_1\ddot{\varphi} + C_{t1}\dot{\varphi} + K_{t1}\varphi \right) + F_{Gdyn} \cdot \frac{d_1}{2} \right) \tag{7}$$

in which F_{Gdyn} is the internal gear dynamic force [30] and d_1, J_1, C_{t1}, K_{t1} are the pitch circle diameter, torsional moment of inertia, damping and stiffness of the driving gear respectively. The simplified, quasi-static form of this equation, ignoring damping, internal gear dynamic and torsional stiffness, can be written as:

$$F_{Sim}^t = \frac{2}{d_1}\left(T_{in}\right) \tag{8}$$

The results of comparison carried in the previous work by Nejad et al. [20] indicate that the simplified method can predict gear transmitted loads with adequate accuracy compared with the MBS method. For each wind speed, the gear transmitted load obtained from simplified or MBS method should be divided in bins or classes [9]. The first bin includes the highest load

value. The bins can be equal size or larger in low wind speed, where the contribution to the fatigue damage is lower. According to IEC 61400-4, this procedure is called as the load duration distribution (LDD) method. The use of LDD method for wind turbine gears and bearings is demonstrated briefly by Niederstucke et al. [10].

4.2- Short-term stress range calculation

A single gear tooth goes in and out of contact in every gear rotation; thus, the root bending stress or surface pitting stress varies in a range from zero to a peak value which does not necessarily correspond with the peaks in the input load range. For instance, the gear tooth root bending stress maximum value occurs when the tooth is at the HPSTC (Highest Point of Single Tooth Contact) point where a single pair of teeth carries the full load and another pair is about to come into contact [7,31,32]. A conservative approach suggested by ISO 6336-6 is to relate the maximum stress range level in each bin to the upper level of the load in that bin. The lower band of the stress range is apparently zero. This method is illustrated in Fig. 6 for the load – transmitted force – bins within F_1 and F_2.

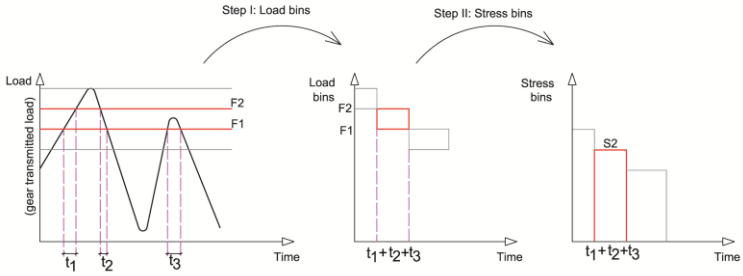

Fig. 6: Creating stress bins from load bins and load time series.

The principal ISO equation for the gear root bending stress S is given as [7]:

$$S = \left\{ \frac{F^t}{bm_n} Y_F Y_S Y_\beta Y_B Y_{DT} \right\} K_A K_V K_{F\beta} K_{F\alpha} K_\gamma \qquad (9)$$

where:

K_A: application factor which takes into account the input or output load variation.

K_V: dynamic factor which represents the influence of internal gear dynamic.

$K_{F\beta}$: face load factor for tooth root stress. It takes into account the uneven load distribution over the gear facewidth due to the misalignment, deflection or geometrical imperfections.

$K_{F\alpha}$: transverse or profile load factor which considers the uneven load distribution over the tooth profile.

K_{γ} : load sharing factor for planetary stage [4]. This factor considers the load sharing between the planets in a planetary gearbox.

F^{t} : gear transmitted load.

b : gear facewidth.

m_{n} : normal module. The gear module is defined as the gear pitch diameter divided by the number of the teeth.

Y_{F} : form factor which takes into account the influence on nominal tooth root stress of the tooth form with load applied at the outer point of single pair tooth contact.

Y_{S} : stress correction factor which corrects the nominal tooth root stress to correspond with the local tooth root stress at the gear root fillet point.

Y_{β} : helix angle factor which considers the effect of helix in helical gears.

Y_{B} : rim thickness factor which adjusts the stress for thin rim gears.

Y_{DT} : deep tooth factor which adjusts the stress for high precision gears.

Table 4 presents the parameters required for stress calculation. Y_{β} , Y_{B} and Y_{DT} are one for all of the case study gears.

Table 4: Geometrical parameters for tooth root stress calculation.

	Sun		Planet/Pinion			Ring/Gear		
	1st	2nd	1st	2nd	3rd	1st	2nd	3rd
b (mm)	620	459	620	459	329	620	459	329
m_{n} (mm)	22	12	22	12	14	22	12	14
Y_{F}	1.60	1.64	1.08	1.03	1.17	0.87	0.87	1.23
Y_{S}	1.76	1.71	2.37	2.45	2.29	2.49	2.55	2.34
K_{γ}	1.10	1.10	1.10	1.10	1.00	1.10	1.10	1.00
$K_{F\beta}$	1.15	1.15	1.15	1.15	1.15	1.15	1.15	1.15
K_{V}	1.05	1.05	1.05	1.05	1.05	1.05	1.05	1.05

4.3- Stress cycle counting method

The number of gear stress cycles is not only dependent on the external load cycles but also is a function of the gear rotational speed. The number of load cycles in each stress bin depends on the time duration of the bin and the gear rotational speed and is calculated from:

$$n_i = \frac{t_i}{60}\omega_i \tag{10}$$

where n_i is the number of stress cycle in stress bin of i, t_i is the time duration of bin i in seconds obtained from the load bin time series – see Fig. 9– and ω_i is the rotational speed of gear in rpm. Fig. 7 shows the stress range bins and corresponding cycle numbers for 1st stage sun gear at various wind speeds.

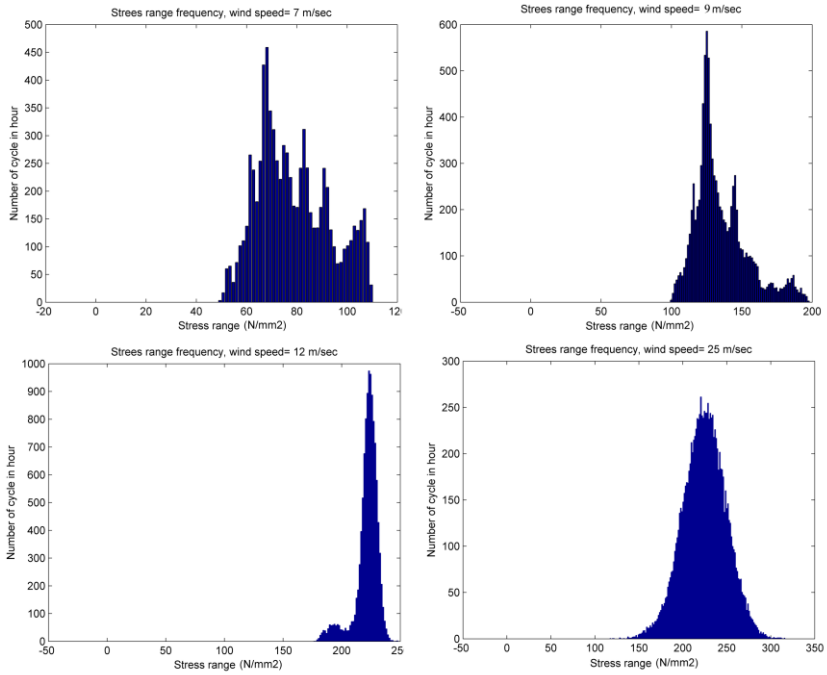

Fig. 7: Stress range vs. number of cycles for 1st stage sun gear at 7, 9, 12 and 25 m/sec.

4.4- Short-term fatigue damage calculation

For each wind speed, the fatigue damage is calculated by Palmgren- Miner linear damage hypothesis:

$$D_c(u) = \sum_i \frac{n_i(u)}{N_{ci}} \tag{11}$$

where n_i is the number of stress cycles in 1-hour with stress range bin of S_i - calculated from equation (10) - and N_{ci} is the characteristic value of the number of stress cycles to failure

with stress range of S_i obtained from the design SN curve given as $N_{ci} = K_c \cdot S_i^{-m}$. K_c and m are obtained from the design SN curve [7]. The SN data are produced from endurance fatigue tests of reference gears by using Pulsator test machines [33] – see section 5.1. The characteristic value of the location parameter, K_c, is calculated from the SN test results and typically corresponds to 97.7% probability of exceedance (mean − two standard deviations for a Gaussian distribution) e.g. [34].

For a wide range of gear materials and heat treatments, ISO 6336-3 and 6336-5 has tabulated the design SN data for both pitting and root bending resistance. For the case study gears made of 16MnCr5 case-hardened, $m = 6.225$ and $\log_{10} K_c = 24.744$ are obtained from ISO 6336-3 for gear tooth root bending.

Apart from direct calculation, equation (11) can be estimated by e.g. [34]:

$$D_c(u) = \sum_i \frac{n_i(u)}{N_{ci}} = \frac{1}{K_c} \sum_i n_i(u) \cdot S_i^m = \frac{N_T}{K_c} \sum_i S_i^m \cdot f(s) \cdot \Delta s \approx \frac{N_T}{K_c} \int_0^\infty S^m \cdot f(s) \cdot ds \qquad (12)$$

where N_T is the number of cycle in the short-term period of 1 hour and $f(s)$ is the stress range distribution.

If $f(s)$ fits the 2-paramters Weibull distribution, the cumulative damage can be obtained analytically by e.g. [34]:

$$D_c(u) = \frac{N_T}{K_c} \int_0^\infty S_i^m \cdot f(s) \cdot ds = \frac{N_T}{K_c} \left\{ a^m \cdot \Gamma\left(1 + \frac{m}{c}\right) \right\} \qquad (13)$$

in which $\Gamma\left(1 + \frac{m}{c}\right)$ is the gamma function and a, c are the Weibull shape and scale parameters of the stress range. This is clearly based on approximation and should be used with caution. Figure 8 shows the difference in damages calculated from the original equation (11) and the approximation, equation (13).

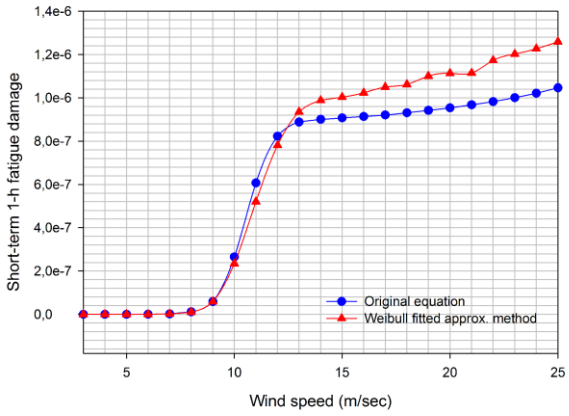

Fig. 8: Gear tooth root bending fatigue damage vs. wind speed for 1st stage sun gear.

The effect of the pitch control system, which is intended to limit the torque above the rated wind speed, is clearly observed in the damage vs. wind speeds figure and the distribution plots of the stress ranges in various wind speeds shown in Fig. 9. The rated wind speed in this case study wind turbine is 11.4 m/sec – see Table 1 for the turbine specifications.

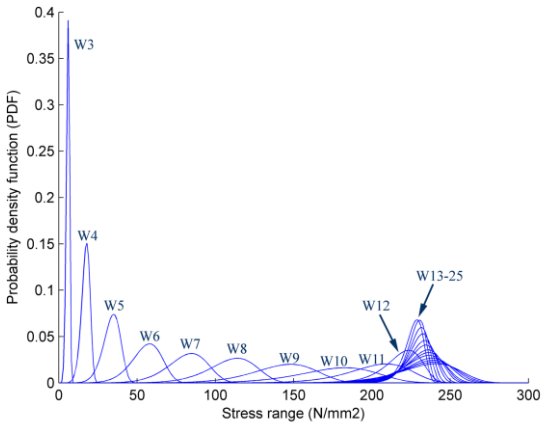

Fig. 9: Stress range probability density function from cut-in to cut-out wind speeds (drawn for the 1st stage sun gear).

4.5- Long-term fatigue damage calculation

In principle, the fatigue damage should include all the short-term damages in the operational wind speed range. The long-term characteristic damage for 20-year design life (D_c^{LT}) is obtained from:

$$D_c^{LT} = \int_{cut-in}^{cut-out} T \cdot D_c(u) \cdot f(u) \cdot du \qquad (14)$$

in which $D_c(u)$ is the short-term 1 hour damages, T the design life e.g. 20-year in hours and $f(u)$ is the probability density function of the mean wind speed. According to IEC 61400-4, the safety factor (S_F) applied to the stress range shall not be less than 1.56 for gear tooth root bending stress. Thus, the design is acceptable if $0.99 < {S_F}^m \cdot D_c^{LT} < 1.00$.

An easier approach is to include the safety factor in the damage limit and to state the fatigue design check as:

$$D_c^{LT} \le \Delta_d = \frac{1}{{S_F}^m} \qquad (15)$$

which leads to $\Delta_d = 0.063$ for the case study gears.

In practice, equation (14) is calculated numerically for discrete wind speeds, often with the span of 1 m/sec. A correction factor should then be applied to compensate for differences between continuous integration and discrete summation of the short-term damages.

In addition to above method, an alternative approach for long-term fatigue calculation is to fit a suitable distribution e.g. Weibull distribution to the long-term stress range. This method, however, is not recommended for gears in pitch controlled wind turbines due to stress range variation below and above rated wind speed. Other distribution models, rather than Weibull distribution, might be applied.

4.6- Case study results

The proposed procedure for the long-term gear tooth root bending fatigue design of wind turbine gears is implemented to the design of a 5 MW case study gearbox. The initial gear parameters are calculated by using ISO 6336-3 and 5 and the upper band of load bins. In each iteration of fatigue damage calculation, the facewidth is modified to fulfil the fatigue criteria described in equation (15).

It is found that the number of bins influence the long-term damage. According to ISO 6336-6, the widely used number of bins is 64. However, as it is shown in Fig. 10, using fewer than 100 bins is rather conservative and leads to bigger gears. This figure is drawn for the first stage sun gear.

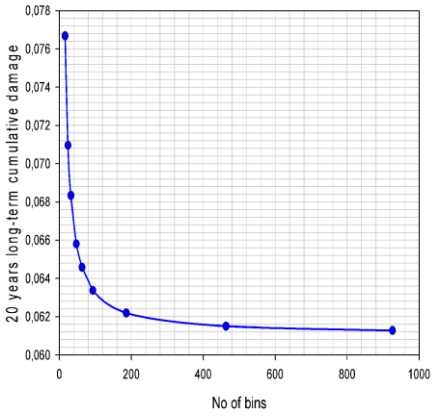

Fig. 10: Long-term damage vs. number of load bins.

It is observed that the wind speeds around rated have the highest contributions in gear root bending fatigue damage – see Fig. 11.

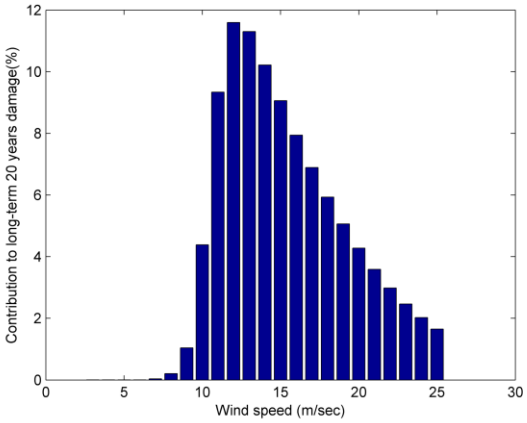

Fig. 11: Contribution of damages in each wind speed to the long-term 20-years damage.

Moreover, the long-term damage calculated from the approximate method by fitting a Weibull distribution to the short-term stress range – equation (11) – is about 8% higher than the results from the direct calculation – equation (13).

The distribution of the damage, and thus the safety factor, is not uniform among the gears in each stage. Table 5 presents the long-term damage in the case study 5 MW gearbox.

Table 5: Long-term 20-years gear tooth root bending fatigue damage.

	1st stage			**2nd stage**			**3rd stage**	
	Sun	Planet	Ring	Sun	Planet	Ring	Pinion	Gear
D^{LT}	0.062	0.023	0.012	0.062	0.021	0.014	0.062	0.030

The results show variations in the damage to the gears. These variations come from geometrical restrictions, differences in stress cycles due to the diverse rotational speeds, and differences in the number of contacts one tooth undergoes in each rotation. The first geometrical restriction for a pair of gears in mesh is to have the same facewidth. However, the minimum facewidth to satisfy the fatigue design criteria for planet or ring gear is less than the sun gear; it is the sun gear which dictates the facewidth for all. The rotational speeds of gears in each stage and between the stages are different, thus their stress cycles are not the same. The last reason, differences in the number of contact one tooth undergoes in each rotation, should be noted during the fatigue design. For instance, for the case study gearbox, a single tooth of the sun gear encounters three contacts in each rotation while a planet gear tooth faces two contacts and the last stage pinion gear tooth only one.

It is also important to underline that the method described here is based on the first gear tooth failure. The gear is considered failed as soon as the fatigue failure occurs in the one gear tooth. The reliability level achieved by this design method is evaluated in the next section.

5. Reliability analysis

In this section, application of the structural reliability method to gears is illustrated. Structural reliability is defined [35] as the ability to fulfil the design purpose for a certain time under specified conditions. The fundamental aim of structural reliability is to estimate the failure probability by explicitly taking into account uncertainties of load/load effect and resistance.

The fatigue failure function $g(\mathbf{X})$ formulated by SN approach is expressed by [34,36]:

$$g(\mathbf{X}) = \Delta - \chi^m D^{LT} \tag{16}$$

where $\mathbf{X}$ denotes the random variables in the load response and resistance. Δ is the failure limit which is in general a random variable with mean value less than one. According to ISO 6336-6 [9] and the experimental works by Yang [40] $\Delta = 1$ is used. χ represents the model uncertainties, equal to:

$$\chi = \chi_{aero}\chi_{dyn}\chi_{sim}\chi_{ben}\chi_{stat} \tag{17}$$

which are detailed in the following section 5.2.

By inserting D^{LT} from equation (14), equation (16) will be written as:

$$g(\mathbf{X}) = 1 - \frac{\chi^m T}{K} \sum_i \left(N_{Ti} \cdot a_i^m \cdot \Gamma\left(1 + \frac{m}{c_i}\right) \right) \cdot f(u_i) \cdot \Delta u_i \tag{18}$$

Let λ be defined as:

$$\lambda = T \cdot \sum_i \left(N_{Ti} \cdot a_i^m \cdot \Gamma\left(1 + \frac{m}{c_i}\right) \right) \cdot f(u_i) \cdot \Delta u_i = K_c \cdot D_c^{LT} \tag{19}$$

then the failure function can be written in logarithm to base 10 form by:

$$g(\mathbf{X}) = \log(K) - m \cdot \log(\chi) - \log(\lambda) \tag{20}$$

In the failure function, K and χ are random variables.

The $g(\mathbf{X}) \le 0$ denotes the failure; thus, the probability of failure is:

$$P_f = P\left[g(\mathbf{X}) \le 0 \right] \tag{21}$$

The failure probability can be uniquely expressed in the form of reliability or safety index, β [37]:

$$\beta = -\Phi^{-1}(P_f) \tag{22}$$

in which $\Phi^{-1}(\ )$ denotes the inverse standard Gaussian cumulative distribution function.

5.1- Gear tooth root strength model

The fatigue resistance, or strength capacity, of gear teeth is a function of gear base material, heat treatment and surface roughness. The fatigue analysis is based on the SN data determined by fatigue testing of gear teeth and the linear damage hypothesis. In general there are two methods for establishing the SN data for gears [8]. In the first method, SN data are derived from endurance tests of gears having dimensions similar to desired gears, under the test conditions which are similar to the intended operating conditions [8]. This is a rather expensive method and is used only in special cases. The second and the most common method is to derive the SN data from endurance tests of reference test gears under reference

test conditions. In this method, the Pulsator test machine is often employed and the gear tooth is loaded at HPSTC point [33].

The load amplitude in Pulsator test is often considered constant [33,38]. The tooth root fillet is the "hot spot" point which is defined as the point where a fatigue crack initiates due to the combined effect of stress fluctuation and the geometry [39]. Final failure for each cycle is the tooth fracture. However, two failure criteria can be considered. First, when the crack initiates at the gear tooth fillet and second when the crack propagates and fracture occurs. According to Bian et al. [38], since the number of cycles between these two phases is very small – about 9000 cycles – compared to the fatigue life of millions of cycles, the difference in fatigue life between these two criteria can be ignored.

It is standard practice to use parametric equations for the derivation of stress concentration factors to obtain surface stress for the actual geometry in gear tooth fillet. This factor is included in equation (9) for the surface stress at the tooth root.

In this case study gearbox, the sun gears, planets and parallel helical gears are case hardened-carburized steel and ring gears are quenched-tempered. All gears are made of 16MnCr5 with average core hardness of 25 HRC (Rockwell hardness scale). The material properties of this alloy steel are listed in Table 7. According to Yang [40], gear tooth root bending strength follows a normal distribution. The $\log(K)$, logarithm of K to base 10, mean and standard deviation are given in the Table 6.

Table 6: Gear material properties.

Property	**Description**	**Value**
S_y	Base material yield strength (N/mm^2)	850
S_{ut}	Base material ultimate strength (N/mm^2)	1200
$\log(K)$	Mean and standard deviation of location parameter in SN curve (N/mm^2)	24.753 , 0.57
m	Slope parameter in SN curve	6.225
E	Young modulus (kN/mm^2)	206
ν	Poisson's ratio	0.3
	Surface hardness (HRC)	59

5.2- Uncertainty models

The uncertainties associated with models for the load and load effect analysis as well as fatigue strength model – see section 5.1 – need to be considered in the reliability analysis. In principle, one needs to run many long-time wind simulations to obtain accurate aerodynamic loads reflecting the various sources of uncertainty by comparing with measurement data or more accurate models. Also, the statistical model and extrapolation in long-term analysis, along with semi-empirical gear load models, induce additional uncertainties which should be considered in reliability analysis.

The model uncertainty is usually defined as [35]:

$$\chi = \frac{X_{true}}{X_{est.}} \tag{23}$$

in which χ represents the model uncertainty of the physical variable X (i.e. aerodynamic load due to wind or gear tooth root fillet stress). The X_{true} is the real value of this variable and $X_{est.}$ is the value obtained from numerical or analytical models. In the reliability analysis, χ is typically modelled as a lognormal random variable. Fig. 12 illustrates the main model uncertainties considered in this paper.

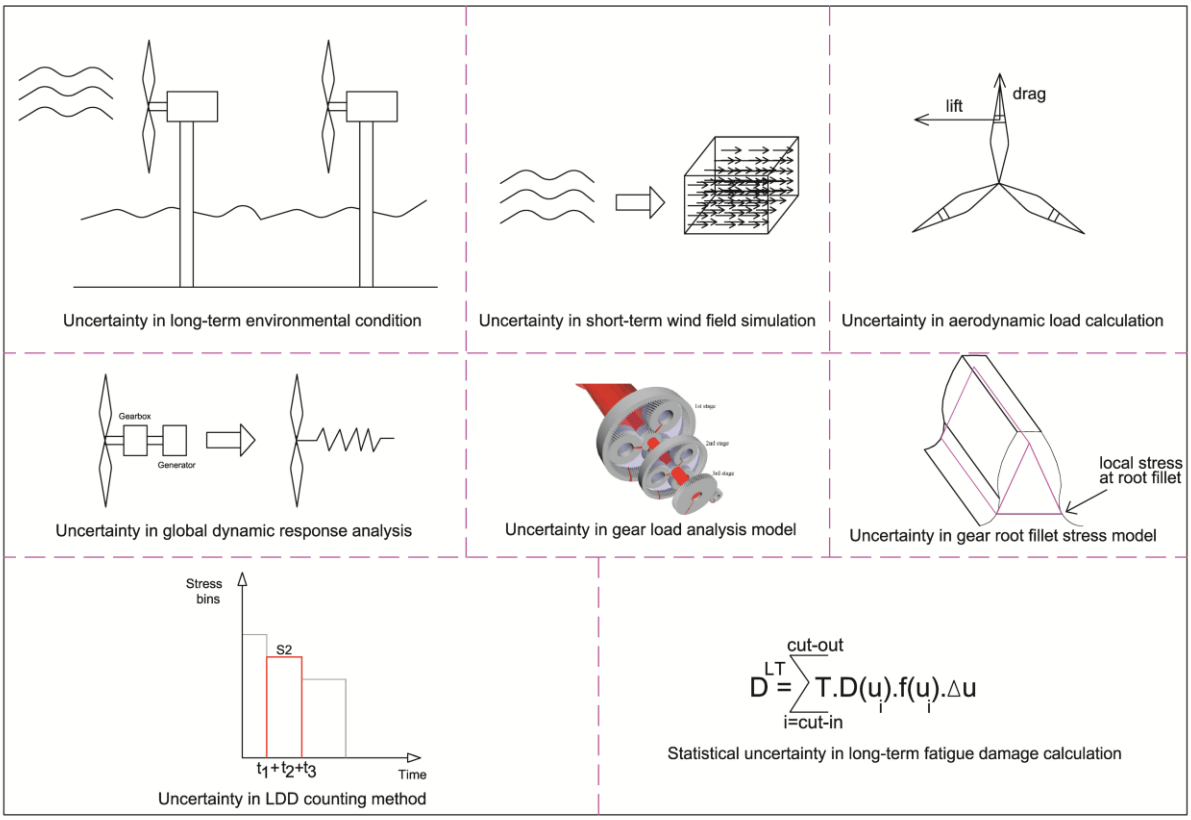

Fig. 12: Illustration of the model uncertainties.

5.2-1. Uncertainty in long-term environmental conditions

In this study, a probabilistic model of mean wind speed in the northern North Sea is used. This model is obtained using the data of a 20 year long continuous time-series of wind measurements covering the years 1973–1999 from the northern North Sea [12].
Wind in this model is characterized by a 1-hour mean wind speed at 10 m above the average sea level and described by 2- parameter Weibull distribution – equation (1).
For fatigue limit state design, Tarp-Johansen et al. [41] have suggested a statistical uncertainty with coefficient of variation (C.O.V) of about 5% in environmental condition model. In this study, the model uncertainty due to the wind model is considered in a conservative way: the turbulence intensity factor is taken as 0.14 for all the wind speeds, according to IEC 61400-1 class B turbine. The turbulence intensity factor represents the deviation of wind speed from the mean value.

5.2-2. Uncertainty in short-term wind field simulation

For each short-term simulation, the turbulence or fluctuation around the mean wind speed over the rotor plane is modelled by Mann uniform shear turbulence model available in HAWC2 for global analysis [14]. This model is a simplification of real turbulence and therefore introduces model uncertainty. The uncertainty in wind field simulation can be reduced by more refined simulation methods such as large eddy simulation (LES) or direct numerical simulation (DNS). Nevertheless, these models normally require long computational time and are not efficient for engineering applications. Another issue is to reduce the associated statistical uncertainty by increasing the number of simulations. In this study, 15 simulations are carried out for each wind speed and the influence of wind field simulation uncertainty is considered in the aerodynamic load calculation uncertainty model.

5.2-3. Uncertainty in aerodynamic load calculation (χ_{aero})

In the HAWC2 [16] program a modified form of blade element momentum (BEM) theory has been used for calculation of the aerodynamic loads on the blades. The lift and drag coefficients uncertainties are accounted in the aerodynamic load uncertainty model. According to empirical and model test investigations by Tarp-Johansen et al. [41] the C.O.V of this model uncertainty for fatigue design is about 10% with mean value of one.

5.2-4. Uncertainty in dynamic response of the turbine (χ_{dyn})

The aerodynamic load on the blades, obtained from the BEM theory, creates load on the main shaft and the drivetrain. The main shaft and other components in the drivetrain are simplified as beam elements which induce model uncertainty. In the global analysis carried by HAWC2, the entire drivetrain is modelled by a single beam element. The χ_{dyn} covers the modelling uncertainty of the dynamic response characteristic of turbine such as natural frequencies, structural damping and stiffness. According to Tarp-Johansen et al. [41], the C.O.V of this uncertainty is around 5% for FLS design with mean value of one.

5.2-5. Uncertainty in simplified model for the gear transmitted load (χ_{sim})

In this paper, the simplified model is used for gear transmitted load calculation. The uncertainty of this model is evaluated by comparison with multibody simulation (MBS) model which is expressed by χ_{sim} :

$$\chi_{sim} = \frac{F_{MBS}^{t}}{F_{Sim}^{t}} \tag{24}$$

in which F_{MBS}^{t} is the gear transmitted force from MBS model and F_{Sim}^{t} is obtained from the simplified method. Table 7 show the log-normal distribution fitting for χ_{sim} in all three stages of the 5 MW case study gearbox.

Table 7: Lognormal distribution parameters for the uncertainty of the simplified gear load model.

	Variable	Distribution	mean	St. dev.
1st stage	χ_{sim}	Lognormal	0.99	0.01
2nd stage			0.99	0.01
3rd stage			0.98	0.02

It appears that the χ_{sim} is relatively small compared to other uncertainties. However, the IEC 61400-4 recommends a minimum C.O.V of 5% shall be considered if calculations indicate lower value.

5.2-6. Uncertainty in gear root stress model (χ_{ben})

Experiments [31,32] as well as 3D FEM contact analyses [42,43] show that the maximum root stress occurs when the contact point is near HPSTC (Highest Point of Single Tooth Contact) where a single pair of teeth carries the full load and another pair is about to come into contact. Along the line of action, a single pair of teeth is under the full loading between LPSTC (Lowest Point of Single Tooth Contact) and HPSTC, while on the rest of the line, two or more teeth are in contact.

In the semi-empirical model proposed by ISO [7] the contact load is applied at HPSTC and the gear tooth is modelled as a triangular beam.

In general, the local stress at the tooth root fillet obtained by FEM are lower than the stresses calculated by the ISO [44]. For gears generated by racks, good agreement is observed between FEM and ISO results [44,45].

The model uncertainty of the ISO analytical method for the gear tooth root stress can be estimated from the comparison with FEM shown in Kawalec's work [44,45]. The model uncertainty of this method can be evaluated by:

$$\chi_{ben} = \frac{\sigma_{Fb\_FEM}}{\sigma_{Fb\_ISO}} \tag{25}$$

in which σ_{Fb_FEM} is the gear tooth root fillet stress obtained from finite element model and σ_{Fb_ISO} is calculated by the ISO model. Based on the Kawalec's work [44,45], the mean and standard deviation of χ_{ben} is estimated to be 0.95 and 0.05 respectively.

5.2-7. Uncertainty in LDD counting method

As discussed in the section 4.2, the conservative approach suggested by ISO 6336-6 is to relate the maximum stress range level in each bin to the upper level of the load in that bin. This uncertainty is design dependent and varies with the gear speed variations and transmitted load fluctuations, but since the upper level of load is chosen, the resultant design is always conservative. The uncertainty of LDD counting method reduces in the steady state or low turbulence conditions. Further experimental work is needed to quantify this uncertainty in different wind conditions.

5.2-8. Uncertainty in long-term fatigue damage (χ_{stat})

The χ_{stat} accounts for the limited number of simulations in long-term fatigue damage calculation. The Tarp-Johansen et al. [46] has suggested a C.O.V value of 5% for this uncertainty. The statistical uncertainty can be reduced by the larger sample size, for instance in the work by Karimirad [47], 2% statistical uncertainty is considered. In this paper the Tarp-Johansen et al. [46] recommendation has been applied.

5.3- Simplified uncertainty treatment in gear fatigue design

The uncertainties associated with the models in different steps that are used to obtain the gear tooth root stress are described in the previous section. The real relation between gear tooth root stress and these uncertainties is very complicated and simplification needs to be made. In order to account for the combined uncertainties in the failure function, some researchers [41,46,48,49] have applied a multiplicative model. In this approach, the relation between the true value of the gear tooth root stress range S_{true} and the calculated value S is expressed by:

$$S_{true} = \chi_{aero}\chi_{dyn}\chi_{sim}\chi_{ben}\chi_{stat}S \tag{26}$$

In this paper the lognormal distribution is selected for all uncertainty distributions. The mean and standard deviation of model uncertainties based on the above discussions are summarized in the Table 8.

Table 8: Uncertainty models.

Uncertainty	Distribution	mean	St. dev.
χ_{aero}	Lognormal	1.00	0.10
χ_{dyn}	Lognormal	1.00	0.05
χ_{sim}	Lognormal	1.00	0.05
χ_{ben}	Lognormal	0.95	0.05
χ_{stat}	Lognormal	1.00	0.05

The CDF of lognormal distribution is given by:

$$F_X(x) = \Phi\left(\frac{\ln x - a}{c}\right) \tag{27}$$

in which $\Phi(\ )$ denotes the standard Gaussian CDF and $\ln$ is the natural logarithm. The a and c are the mean and standard deviation of $\ln x$ respectively.

5.4- Reliability analysis results and discussion

The reliability analysis is performed by the first-order reliability method (FORM) as described by Madsen et al. [37] using the Proban software [50].

Table 9 and Fig. 13 show the life time 20-years reliability index and failure probability of gears. The importance factors for the uncertainty models and the random variable are also listed. The importance factor expresses relative importance of different uncertainties on the reliability [35] and mathematically is defined by [35,51]:

$$\alpha_{\mu} = \frac{\partial \beta}{\partial \mu} \tag{28}$$

where μ is the mean value of the random variables and α_{μ} is the importance factor.

Table 9: Service life reliability index, probability of failure and importance factors.

Stage	Gear	β	$P_f\left(\times 10^{-2}\right)$	Importance factor (%)					
				χ_{aero}	χ_{dyn}	χ_{sim}	χ_{ben}	χ_{stat}	$\log(K)$
1	Sun	2.21	1.35	18.6	4.7	4.7	4.7	4.7	62.7
	Planet	2.90	0.19	18.6	4.7	4.7	4.7	4.7	62.7
	Ring	3.35	0.01	18.6	4.7	4.7	4.7	4.7	62.7
2	Sun	2.21	1.35	18.6	4.7	4.7	4.7	4.7	62.7
	Planet	2.96	0.15	18.6	4.7	4.7	4.7	4.7	62.7
	Ring	3.24	0.06	18.6	4.7	4.7	4.7	4.7	62.7
3	Pinion	2.21	1.35	18.6	4.7	4.7	4.7	4.7	62.7
	Gear	2.72	0.33	18.6	4.7	4.7	4.7	4.7	62.7

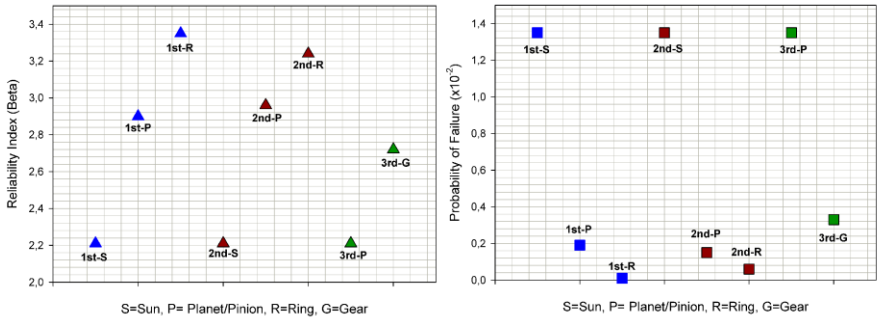

Fig. 13: Service life reliability index and probability of failure for gears in a 5 MW gearbox.

Fig. 14 illustrates the 20-years probability of failure versus long-term fatigue damage for gears in all stages.

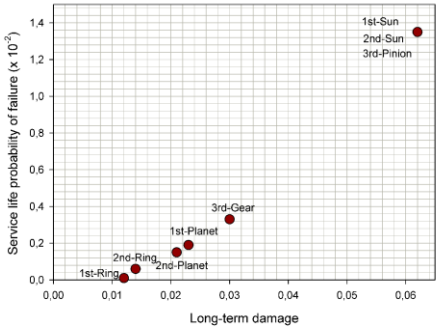

Fig. 14: Service life probability of failure vs. long-term damage for gears in a 5 MW gearbox.

The results show that the gears designed with the IEC 61400-4 recommended safety factor of 1.56 on stress – or 1.56^m on life – lead to the minimum reliability of 2.21. The question that may arise here is what level of reliability is acceptable for gears in fatigue design? This level is the so called target reliability in a probabilistic or semi-probabilistic design. In the wind turbine design codes, the target reliability is not explicitly defined for gears.

The current annual failure rate of the wind turbine gearboxes is about 0.15 per gearbox [52] implying a reliability level of 1.04. However, the source of this relatively high failure rate among the gearbox components is not clearly known. Whether the gear failure is the cause of this short life or bearing damage, is not clearly identified.

Nevertheless, the choice of target reliability level should balance the cost of safety measures and the consequences of failure [53]. The IEC 61400-1 has classified wind turbine gearboxes as class 2 components with respect to the potential consequences of failures. The class 2 components are “non fail-safe” components whose failures may lead to the failure of a major part of a wind turbine [15].

6. Concluding remarks

This paper describes a long-term gear tooth root bending fatigue damage calculation method for gears in wind turbines. The ISO 6336-6 method for gears in general use has been used as the basis and is further adapted and customized for gears in wind turbine applications. First, the short-term load and stress ranges are discussed. Second, the cumulative fatigue damage is

calculated by the Palmgren-Miner hypothesis of linear damage and gear's SN curve data. In addition to the direct damage calculation method, an analytical method based on the distribution of stress ranges is discussed. The uncertainty of this approach increases in higher wind speeds. Third, the long-term damage is finally obtained by taking in account the long-term wind speed distribution and required IEC 61400-4 safety factor. It is shown that the number of stress bins affects the calculated damage. The cumulative damage calculated by 100 and more equal bins leads to the smaller gears than the 64 bins used by ISO 6336-6. Most importantly, it is observed that the wind speeds around rated speed contribute more than other wind speeds in the gear fatigue damage. In the earlier work by Nejad et al. [20] it is shown that the wind speeds near cut-out hold the highest contributions in extreme loads on gears in normal operations, while for fatigue design, the wind speeds near rated are those with higher impacts.

Furthermore, the sun gears in planetary stages and pinion in parallel helical stage are those with the highest damage. This is primarily due to their higher number of cycles and lower number of teeth comparative to planets, rings and gear wheel in the last stage.

The reliability analysis is then carried out by the first-order reliability method (FORM) and the reliability index of gears in each stage is presented. It is followed by a detailed treatment of the uncertainties in the models for load/load effect and strength analysis.

It is emphasized that the reliability level demonstrated herein is wind turbine and site-specific and only applicable to gear tooth root stress. For different sites – other than the Northern North Sea – and different wind turbine sizes, other values may result. It is therefore proposed to devote future work to investigations of gearboxes in different sites and sizes with the aim to develop a FLS reliability-based design code for wind turbine gearboxes. Moreover, further works are needed in uncertainty modelling and reliability analysis of the gearbox as a system of components.

Acknowledgements

The authors wish to acknowledge the financial support from Research Council of Norway through Norwegian Research Centre for Offshore Wind Technology (Nowitech) and Centre for Ships and Ocean Structures (CeSOS). The first author would also like to thank Dr. Y. Xing, E. Bachynski from CeSOS and Dr. Y. Guo from Gearbox Reliability Collaborative

(GRC) at US National Renewable Energy Laboratory (NREL), for discussions on wind turbine gearbox modelling in a multibody environment and constructive comments.

References

[1] Crowther A., Ramakrishnan V., Zaidi N. A., Halse C. Sources of time-varying contact stress and misalignments in wind turbine planetary sets. Wind Energy; 2011: 14, 637-651.

[2] Musial W., Butterfield S., McNiff B. Improving wind turbine gearbox reliability. Proceeding of European Wind Energy Annual Conference, EWEA 2007, 7-10 May, Milan, Italy.

[3] International Organization for Standardization, Wind Turbines – Part 4: Standard for Design and Specification of Gearboxes, ISO/IEC 81400-4:2005, ISO Geneva, Switzerland, February 2005.

[4] International Electrotechnical Commission, IEC 61400-4: Wind turbines – Part 4: Standard for design and specification of gearboxes, Dec. 2012.

[5] International Organization for Standardization, ISO 6336-1: Calculation of load capacity of spur and helical gears – Part 1: Basic principles, introduction and general influence factors, 2006.

[6] International Organization for Standardization, ISO 6336-2: Calculation of load capacity of spur and helical gears – Part 2: Calculation of surface durability (pitting), 2006.

[7] International Organization for Standardization, ISO 6336-3: Calculation of load capacity of spur and helical gears – Part 3: Calculation of tooth bending strength, 2006.

[8] International Organization for Standardization, ISO 6336-5: Calculation of load capacity of spur and helical gears – Part 5: Strength and quality of material, 2003.

[9] International Organization for Standardization, ISO 6336-6: Calculation of load capacity of spur and helical gears – Part 6: Calculation of service life under variable load, 2006.

[10] Niederstucke B., Anders A., Dalhoff P., Grzybowski R. Load data analysis for wind turbine gearboxes, in "Final Report, ELA - Enhanced Life Analysis of Wind Power Systems, 2003", Germanischer Lloyd WindEnergie GmbH. Available online at: http://www.germanlloyd.org/pdf/nst_paris.pdf

[11] Dong W., Xing Y., Moan T., Gao Z. Time domain-based gear contact fatigue analysis of a wind turbine drivetrain under dynamic conditions; International Journal of Fatigue: 2013, 48, 133-146.

[12] Johannessen K., Meling T. S., Haver S. Joint distribution for wind and waves in the Northern North sea. International Journal of Offshore and Polar Engineering; 2002: 12, 1, 1-9.

[13] Ronold K. O., Larsen G. C. Variability of extreme flap loads during turbine operation, 1999 European wind energy conference. 1-5 March, 1999 Nice, France.

[14] International Electrotechnical Commission, IEC 61400-3: Wind turbines – Part 3: Design requirements for offshore wind turbines, 2009.

[15] International Electrotechnical Commission, IEC 61400-1: Wind turbines – Part 1: Design requirements, 2005.

[16] HAWC2, Aero-servo-elastic calculation code for horizontal axis wind turbine, Risoe centre, Denmark Technical University (DTU), Denmark.

[17] Nejad A. R., Xing Y., Guo Y., Keller J., Gao Z., Moan T. Effect of floating sun gear in wind turbine planetary gearbox with geometrical imperfections, Wind Energy, under review, 2013.

[18] Jonkman J., Butterfield S., Musial W., Scott G. Definition of a 5-MW reference wind turbine for offshore system development. US National Renewable Energy Laboratory report no. NREL/TP-500-38060, Feb. 2009.

[19] Xing Y., Moan T. Multi-body modelling and analysis of a planet carrier in a wind turbine gearbox. Wind Energy, 2012 (DOI: 10.1002/we.1540).

[20] Nejad A. R., Gao Z., Moan T. Long-term analysis of gear loads in fixed offshore wind turbines considering ultimate operational loadings. Energy Procedia; 2013: 35, 187-197.

[21] Xing Y. Modelling and analysis of the gearbox in a floating spar-type wind turbine. Ph.D. thesis, Norwegian University of Science and Technology, Department of Marine Technology, 2013.

[22] Peeters J. Simulation of dynamic drive train loads in a wind turbine. Ph.D. thesis, Katholieke Universiteit Leuven, Belgium, 2006.

[23] Parker R.G., Agashe V., Vijayakar S.M. Dynamic response of a planetary gear system using a finite-element contact mechanics model. Transaction of ASME, Journal of Mechanical Design; 2000: 122, 304–311.

[24] Kahraman A., Kharazi A., Umrani M. A deformable-body dynamic analysis of planetary gears with thin rims. Journal of Sound and Vibration; 2003:262, 752–768.

[25] Yuksel C., Kahraman A. Dynamic tooth loads of planetary gear sets having tooth profile wear. Mechanism and Machine Theory;2004:39,695-715.

[26] Multi Body System software, SIMPACK, www.simpack.de.

[27] Oyague F. Gearbox modelling and load simulation of a baseline 750-kW wind turbine using state-of-the-art simulation codes, National Renewable Energy Laboratory, NREL/TP-500-41160, 2009.
[28] Parker R. G., Vijayakar S. M., Imajo T. Non-linear dynamic response of a spur gear pair: modeling and experimental comparisons. Journal of Sound and Vibration; 2000: 237 (3), 435-455.
[29] Parker R. G. Gear dynamic short course notes. Norwegian University of Science and Technology (NTNU), April 2011.
[30] Nejad A. R., Xing Y., Moan T. Gear train dynamics in large offshore wind turbines. The ASME 2012 11th Biennial Conference on Engineering Systems Design and Analysis, Nantes, France; 2012.
[31] American Gear Manufacturers Association, AGMA 908-B89: Geometry factors for determining the pitting resistance and bending strength of spur, helical and herringbone gear teeth, 1999.
[32] Spitas V., Spitas C. Numerical and experimental comparative study of strength-optimised AGMA and FZG spur gears. Acta Mechanica; 2007: 193, 113-126.
[33] Shaw B. A., Aylott C., Brimble K. The role of residual stress on the fatigue strength of high performance gearing, International Journal of Fatigue; 2003: 25, 1279-1283.
[34] Naess A., Moan T. Stochastic dynamics of marine structures. Cambridge University Press, 2012.
[35] Moan T. Structural risk and reliability analysis. Lecture notes, Norwegian University of Science and Technology (NTNU), Department of Marine Technology, 2008.
[36] Ronold K. O., Lotsberg I. On the estimation of characteristic SN curves with confidence; Marine Structures: 2012, 27, 29-44.
[37] Madsen H. O., Krenk S., Lind N.C. Methods of structural safety. Dover Publications, 2006.
[38] Bian X. X., Zhou G., Li W., Tan J. Z. Investigation of bending fatigue strength limit of alloy steel gear teeth, Proc. IMechE Part C, 2011, 226, 615-625.
[39] DNV-RP-C203, Fatigue design of offshore steel structures, Det Norske Veritas, Norway, 2011.
[40] Yang Q. J. Fatigue test and reliability design of gears, International Journal of Fatigue; 1996: 18(3), 171-177.

[41] Tarp-Johansen N.J. Examples of fatigue lifetime and reliability evaluation of larger wind turbine components. Riseo report R-1418, Riso National Laboratory, Denmark, 2003.
[42] Chen Y. C., Tsay C. B. Stress analysis of a helical gear set with localized bearing contact. Finite Element in Analysis and Design; 2002: 38, 707-723.
[43] Rao R. M., Muthuveerapan G. Finite element modelling and stress analysis of helical gear teeth. Computers & Structures; 1994: 49(6), 1095-1106.
[44] Kawalec A., Wiktor J., Ceglarek D. Comparative analysis of tooth-root strength using ISO and AGMA standards in spur and helical gears with FEM-based verification. ASME Journal of Mechanical Design; 2006:128, 1141-1158.
[45] Kawalec A., Wiktor J. Tooth root strength of spur and helical gears manufactured with gear-shaper cutters. ASME Journal of Mechanical Design; 2008:130.
[46] Tarp-Johansen N.J., Madsen P.H., Frandsen S.T. Partial safety factors for extreme load effects, proposal for the 3rd Ed. of IEC 61400: Wind Turbine Generator Systems-Part 1: Safety Requirements. Riseo report R-1319, Riseo National Laboratory, 2002.
[47] Karimirad, M. and Moan, T. Stochastic dynamic response analysis of a tension leg spar-type offshore wind turbine. Wind Energy, 2012. doi: 10.1002/we.1537.
[48] Dong W., Moan T., Gao Z. Fatigue reliability analysis of the jacket support structure for offshore wind turbine considering the effect of corrosion and inspection. Reliability Engineering & System Safety; 2012: 106, 11-27.
[49] Sigurdsson G, Cramer E. Guideline for offshore structural reliability analysis: examples for jacket platforms. Report no. 95-3204, 1996, Det Norske Veritas. Oslo, Norway.
[50] Proban version 5.1-01, 2010, Det Norske Veritas Software, Norway.
[51] Proban theory manual, 2004, Det Norske Veritas Software, Norway.
[52] Tavner P.J., Van Bussel G.J.W., Koutoulakos E. Reliability of different wind turbine concepts with relevance to offshore application. European Wind Energy Conference (EWEC), 31 March – 3 April, 2008, Brussels, Belgium.
[53] International Organization for Standardization, ISO 2394: General principles on reliability for structures, 1998.